

Characterization of Biaxial Materials Using a Partially-Filled Rectangular Waveguide

J. Tang¹, B. Crowgey¹, O. Tuncer¹, E. Rothwell¹, B. Shanker¹, L. Kempel¹, and M. Havrilla²

¹Department of Electrical and Computer Engineering
Michigan State University, East Lansing, MI 48824, USA
rothwell@egr.msu.edu

²Department of Electrical and Computer Engineering
Air Force Institute of Technology, Wright-Patterson Air Force Base, OH, 45342
Michael.Havrilla@afit.edu

Abstract— A technique is proposed to measure the permittivity and permeability parameters of a sample of biaxial material placed into a rectangular waveguide. By constructing the material as a cube, only a single sample is required to find all six material parameters. The sample is inserted into the waveguide in multiple orientations, and the transmission and reflection coefficients of the sample region are measured using a vector network analyzer. The material parameters are then found by equating the measured S-parameters to those determined theoretically using a mode-matching technique. The theoretical details are outlined and the extraction process is described. A stacked dielectric cube is characterized experimentally to demonstrate the feasibility of the approach, and results are compared to those obtained using a reduced-aperture waveguide technique.

Index Terms – Anisotropic, biaxial, material measurement, permeability, permittivity, and waveguide.

I. INTRODUCTION

Engineered materials, formed from composites of various constituents with both dielectric and magnetic properties, are gaining interest for use in antenna apertures due to their useful electromagnetic properties [1, 2]. These materials are often anisotropic, and their constitutive

parameters are hard to predict theoretically. Thus it is important to develop methods to accurately characterize the behavior of anisotropic materials experimentally, so that the constitutive parameters may be used in the analysis and design of antenna systems.

Rectangular waveguide systems are often used to measure the electromagnetic properties of materials due to high signal strength, ease of sample preparation, and the ability to analyze the sample interaction analytically [3]. The authors have recently developed a method for characterizing the properties of biaxially anisotropic materials using a reduced-aperture waveguide system [4]. By using a sample holder of cubical shape, a single sample of biaxial material may be measured in three different orientations, providing the required number of reflection and transmission measurements to determine the six unique constitutive parameters. The fields in the sample region are computed analytically, and the mode-matching approach is used to determine the theoretical S-parameters of the cascaded system consisting of the sample holder and the empty waveguide transitions. This technique has the drawbacks that the sample must fit tightly within the conducting sample holder (to preclude air gaps), the restricted aperture of the sample holder reduces the energy transmitted through the sample, and a special sample holder must be constructed.

This paper introduces an alternative technique that doesn't require a special sample holder. In this technique a cubical sample is inserted directly into a full-aperture waveguide, leaving spaces on each side of the sample. The sample is centered within the guide cross section, and mode-matching techniques are again used to find the S-parameters. This approach eliminates the presence of gaps along the sidewalls (although not along the top and bottom walls), reduces reflections from the conducting restriction, and does not require a special sample holder. Drawbacks include accurately centering the sample in the guide, and dealing with a more complicated field structure in the sample region, including finding the modal propagation constants by solving a transcendental equation.

II. THEORETICAL S-PARAMETERS FOR A CUBICAL BIAxIAL MATERIAL SAMPLE IN A RECTANGULAR WAVEGUIDE

Dependable extraction of the biaxial properties of a material sample depends on having an accurate model for the theoretical S-parameters of the measurement system. The system considered here is designed in such a way that simple mode-matching techniques can be used to find the S-parameters with a computational accuracy that is easily quantified [5].

Consider the system shown in Fig. 1. A cubical sample of material is centered within the cross-section of a rectangular waveguide such that the cross-sectional view is shown in Fig. 2. The material is assumed to be biaxial along the orthogonal axes A , B , and C , such that the tensor permittivity and permeability are given by,

$$\epsilon = \epsilon_0 \begin{bmatrix} \epsilon_A & 0 & 0 \\ 0 & \epsilon_B & 0 \\ 0 & 0 & \epsilon_C \end{bmatrix} \quad (1)$$

and

$$\mu = \mu_0 \begin{bmatrix} \mu_A & 0 & 0 \\ 0 & \mu_B & 0 \\ 0 & 0 & \mu_C \end{bmatrix}, \quad (2)$$

respectively, where ϵ_A , μ_A , etc., are relative parameters. A TE_{10} rectangular waveguide mode is assumed to be incident upon the sample from the region $z < 0$, as shown in Fig. 3. Due to the material discontinuities at the sample interfaces,

an infinite spectrum of empty waveguide modes is reflected back into this region, an infinite spectrum of modes is created in the sample region, $0 \leq z \leq d$, and an infinite spectrum of modes is transmitted into the region $z > d$. The empty waveguide sections on the sending and receiving ends are assumed to be of sufficient length that only the dominant empty waveguide TE_{10} mode propagates to the ends of the sections. Thus, dominant-mode reflection and transmission coefficients can be measured at these ports using a vector network analyzer, and the S-parameters of the sample determined by shifting these measurements to the sample planes $z = 0$ and $z = d$. To determine the biaxial material properties, the theoretical S-parameters are needed at these planes.

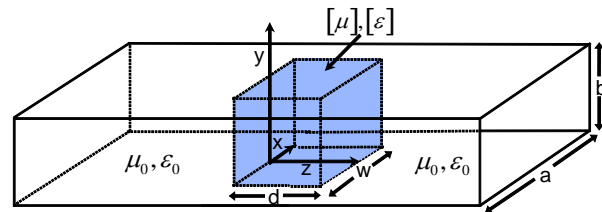


Fig. 1. Cubical sample of biaxial material centered inside a rectangular waveguide.

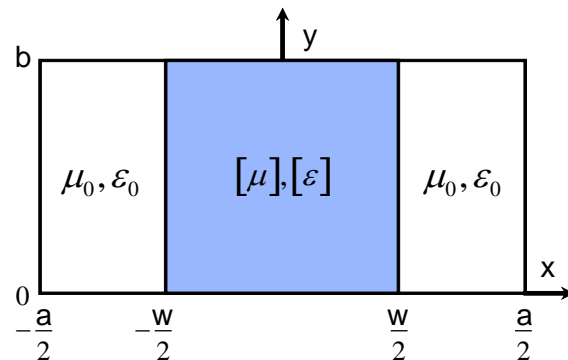


Fig. 2. Cross-sectional view of the sample inside the waveguide.

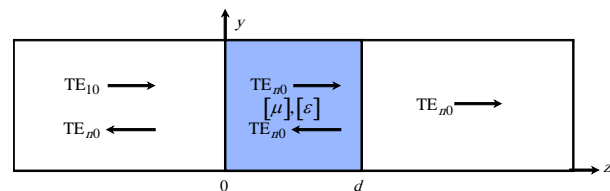


Fig. 3. Side view of the sample inside the waveguide showing the presence of higher-order modes in each region.

Since the electric field of the dominant TE₁₀ mode of the empty guide is even about x , the incident field will only couple to modes with a similar symmetry. The field structure of the empty waveguide modes is well known [6], and it is easily seen that only modes of the type TE _{n 0} will be excited in the empty guides. Thus, the transverse fields in the region $z < 0$ may be expanded as,

$$E_y(x, z) = a_1^i \bar{E}_1(x) e^{-j\bar{\beta}_1 z} + \sum_{n=1}^N a_n^r \bar{E}_n(x) e^{+j\bar{\beta}_n z} \quad (3)$$

$$H_x(x, z) = -a_1^i \bar{H}_1(x) e^{-j\bar{\beta}_1 z} + \sum_{n=1}^N a_n^r \bar{H}_n(x) e^{+j\bar{\beta}_n z}, \quad (4)$$

while the field in the region $z > d$ may be written as,

$$E_y(x, z) = \sum_{n=1}^N a_n^t \bar{E}_n(x) e^{-j\bar{\beta}_n(z-d)} \quad (5)$$

$$H_x(x, z) = -\sum_{n=1}^N a_n^t \bar{H}_n(x) e^{-j\bar{\beta}_n(z-d)}. \quad (6)$$

Here a_1^i is the known amplitude of the incident TE₁₀ mode, while a_n^r and a_n^t are modal amplitudes to be determined by applying appropriate boundary conditions at the interfaces between the samples and the empty waveguide sections. Once these are found, the theoretical S-parameters are given by,

$$S_{11}^T = \frac{a_1^r}{a_1^i} \quad (7)$$

$$S_{21}^T = \frac{a_1^t}{a_1^i}. \quad (8)$$

In equations (3) to (6), $\bar{\beta}_n$ is the real phase constant of the TE _{n 0} mode given by,

$$\bar{\beta}_n = \sqrt{k_0^2 - \bar{k}_{c,n}^2} \quad (9)$$

with $k_0 = \omega\sqrt{\mu_0\epsilon_0}$ is the free-space wave number, and $\bar{k}_{c,n}$ the cutoff wavenumber,

$$\bar{k}_{c,n} = \frac{n\pi}{a}, \quad n = 1, 2, 3, \dots \quad (10)$$

Also in equations (3) to (6), the field structure of the empty waveguide modes is given by,

$$\bar{E}_n(x) = -\frac{j\omega\mu_0}{\bar{k}_{c,n}} \sin\bar{k}_{c,n} \left(x - \frac{a}{2}\right) \quad (11)$$

$$\bar{H}_n(x) = \frac{\bar{E}_n}{\bar{Z}_n}, \quad (12)$$

where \bar{Z}_n is the TE-wave impedance

$$\bar{Z}_n = \frac{\omega\mu_0}{\bar{\beta}_n}. \quad (13)$$

The field structure of the waveguide modes in the sample region is somewhat more complicated. Assuming that the biaxial cube is aligned so that the axes A , B , and C lie along some choice of the directions x , y , and z , the fields within the region $0 \leq z \leq d$ may be expanded as,

$$E_y(x, z) = \sum_{n=1}^N [a_n^+ e^{-j\beta_n z} + a_n^- e^{+j\beta_n z}] E_n(x) \quad (14)$$

$$H_x(x, z) = \sum_{n=1}^N [-a_n^+ e^{-j\beta_n z} + a_n^- e^{+j\beta_n z}] H_n(x), \quad (15)$$

where a_n^+ and a_n^- are amplitudes to be determined by application of the boundary conditions at $z = 0$ and $z = d$. Here the modal fields are given for $x > 0$ by,

$$E_n(x) = \begin{cases} E_n^I(x), & 0 \leq x \leq \frac{w}{2} \\ E_n^{II}(x), & \frac{w}{2} < x \leq \frac{a}{2} \end{cases} \quad (16)$$

$$H_n(x) = \begin{cases} H_n^I(x), & 0 \leq x \leq \frac{w}{2} \\ H_n^{II}(x), & \frac{w}{2} < x \leq \frac{a}{2} \end{cases} \quad (17)$$

where

$$E_n^I(x) = \frac{j\omega\mu_z}{k_{c,n}^I} \cos(k_{c,n}^I x), \quad (18)$$

$$E_n^{II}(x) = -\frac{j\omega\mu_0}{k_{c,n}^{II}} \sin\left(k_{c,n}^{II} \frac{d}{2}\right) \frac{\sin k_{c,n}^{II} \left(x - \frac{a}{2}\right)}{\cos k_{c,n}^{II} \left(\frac{d-a}{2}\right)}, \quad (19)$$

$$H_n^I(x) = \frac{E_n^I(x)}{Z_n^I}, \quad H_n^{II}(x) = \frac{E_n^{II}(x)}{Z_n^{II}}, \quad (20)$$

with

$$Z_n^I = \frac{\omega\mu_x}{\beta_n}, \quad Z_n^{II} = \frac{\omega\mu_0}{\beta_n}. \quad (21)$$

These fields are found by solving the wave equation for a biaxial medium [7],

$$\left[\frac{\partial^2}{\partial x^2} + \frac{\mu_z}{\mu_x} (\omega^2 \mu_x \epsilon_y - \beta^2) \right] H_z(x, z) = 0 \quad (22)$$

and applying the boundary conditions at the interfaces $x = a/2$ and $x = w/2$. Note that because of symmetry, the boundary conditions at $x = -a/2$ and $x = -w/2$ are satisfied automatically.

The complex propagation constants β_n are found by solving the transcendental equation,

$$\mu_0 k_{c,n}^I \sin\left(k_{c,n}^I \frac{w}{2}\right) \sin\left(k_{c,n}^{II} \frac{a-w}{2}\right) = \mu_z k_{c,n}^{II} \cos\left(k_{c,n}^I \frac{w}{2}\right) \cos\left(k_{c,n}^{II} \frac{a-w}{2}\right) \quad (23)$$

where the cutoff wavenumbers are related to the complex propagation constants by,

$$\begin{aligned} (k_{c,n}^I)^2 &= \frac{\mu_z}{\mu_x} (\omega^2 \mu_x \varepsilon_y - \beta_n^2) \\ (k_{c,n}^{II})^2 &= k_0^2 - \beta_n^2. \end{aligned} \quad (24)$$

It is not as straightforward to number the modes in the partially-filled guide as it is to number the modes in the empty waveguide extensions. One approach is to start with the solution for β_n under the condition $w = 0$, which is given by equations (9) and (10) since the sample region is empty, and then slowly increase the width of the sample, solving for β_n at each step using the previous solution as an initial guess. Then the modes can be numbered according to the starting empty waveguide mode. This is the approach suggested in [8] for thin samples. However, as the sample width increases, modes may switch between propagating and evanescent, and solving equation (23) using previous results as initial guesses becomes problematic. Instead, when the material loss is not too high, the following approach can be used. First the imaginary parts of the material constants are set to zero (implying a lossless material). Then the real values of β are found by looking for zero crossings of equation (23) between $\beta = 0$ and $\beta = \omega \sqrt{\mu_x \varepsilon_y}$. These are the propagating modes, and are assigned the index n according to the order of the zero crossing. Next β is replaced by $-j\delta$ in equation (23), and real values of δ are found by looking for zero crossings starting from $\delta = 0$ and continuing until a prescribed number of modes have been found. These are the evanescent modes, and they are numbered continuing after the highest order propagating mode. Finally, the imaginary parts of the material parameters are restored, and the zero crossing values found earlier for β and δ are used as initial guesses in a Newton's method root search (possibly with a small imaginary perturbation) to find the complex propagation constants for both the propagating and the evanescent modes.

The unknown modal amplitudes are found by enforcing continuity of E_y and H_x at the interfaces $z = 0$ and $z = d$,

$$a_1^i \bar{E}_1(x) + \sum_{n=1}^N a_n^r \bar{E}_n(x) = \sum_{n=1}^N [a_n^+ + a_n^-] E_n(x) \quad (25)$$

$$-a_1^i \bar{H}_1(x) + \sum_{n=1}^N a_n^r \bar{H}_n(x) = \sum_{n=1}^N [-a_n^+ + a_n^-] H_n(x), \quad (26)$$

$$a_n^- e^{+j\beta_n d} E_n(x) = \sum_{n=1}^N a_n^t \bar{E}_n(x), \quad (27)$$

$$\begin{aligned} \sum_{n=1}^N [-a_n^+ e^{-j\beta_n d} + a_n^- e^{+j\beta_n d}] H_n(x) = \\ - \sum_{n=1}^N a_n^t \bar{H}_n(x). \end{aligned} \quad (28)$$

Note that, for convenience, the same number of modes, N , is used in the empty waveguide and sample holder regions.

Equations (25) to (28) are a system of functional equations. They may be transformed into a system of linear equations by applying appropriate testing operators as follows. First, equation (25) is multiplied by $\bar{E}_m(x)$ and integrated between 0 and $a/2$. Next, equation (26) is multiplied by $\bar{H}_m(x)$ and integrated between 0 and $a/2$. Then equation (27) is multiplied by $\bar{E}_m(x)$ and integrated between 0 and $a/2$. Finally, equation (28) is multiplied by $\bar{H}_m(x)$ and integrated between 0 and $a/2$. Note that all integrals can be computed in closed form. The result is a linear system of $4N \times 4N$ equations of the form,

$$\begin{bmatrix} -C_{mn} & D_{mn} & D_{mn} & 0 \\ E_{mn} & F_{mn} & -F_{mn} & 0 \\ 0 & D'_{mn} & D''_{mn} & -C_{mn} \\ 0 & -F'_{mn} & F''_{mn} & E_{mn} \end{bmatrix} \begin{bmatrix} a_n^r \\ a_n^+ \\ a_n^- \\ a_n^t \end{bmatrix} = a_1^i \begin{bmatrix} C_{m1} \\ E_{m1} \\ 0 \\ 0 \end{bmatrix} \quad (29)$$

where each of the quantities C_{mn} , D_{mn} , etc., are $N \times N$ submatrices, and a_n^r , a_n^+ , etc., are the unknown modal coefficients. Once the matrix of equation (29) has been solved, equations (7) and (8) can be used to compute the desired S-parameters.

III. EXTRACTION PROCEDURE

Since there are six independent complex quantities to determine, $(\varepsilon_A, \varepsilon_B, \varepsilon_C, \mu_A, \mu_B, \mu_C)$, the extraction process requires a minimum of six complex measurements. These may be obtained by measuring S_{11} and S_{21} with the material axes A , B , and C aligned along three properly chosen directions. Consider the orientations,

$$(A, B, C) \rightarrow (x, y, z) \quad (30)$$

$$(A, B, C) \rightarrow (z, x, y), \quad (31)$$

$$(A, B, C) \rightarrow (y, z, x). \quad (32)$$

Measurement under these orientations gives the S-parameters $(S_{11,1}^{\text{meas}}, S_{21,1}^{\text{meas}})$, $(S_{11,2}^{\text{meas}}, S_{21,2}^{\text{meas}})$, $(S_{11,3}^{\text{meas}}, S_{21,3}^{\text{meas}})$, respectively. The material parameters can be found by solving the system of six nonlinear equations in six complex unknowns,

$$S_{11,n}^{\text{thy}}(\varepsilon_A, \varepsilon_B, \varepsilon_C, \mu_A, \mu_B, \mu_C) - S_{11,n}^{\text{meas}} = 0$$

$$n = 1, 2, 3 \quad (33)$$

$$S_{21,n}^{\text{thy}}(\varepsilon_A, \varepsilon_B, \varepsilon_C, \mu_A, \mu_B, \mu_C) - S_{21,n}^{\text{meas}} = 0$$

$$n = 1, 2, 3. \quad (34)$$

It may be difficult to solve this set of equations using standard methods such as Newton's method, since extremely accurate initial guesses may be required. Alternatively, a subset of the material parameters may be found using fewer equations and then these parameters may be used as known quantities to solve for the remaining parameters. This approach is possible since only the three parameters ε_y , μ_x , and μ_z appear at any given orientation.

Although many possible measurement combinations are possible, the results shown here were obtained using a three-step process. First, measurements are made with the orientations,

$$(A, B, C) \rightarrow (x, y, z) \quad (35)$$

$$(A, B, C) \rightarrow (-z, y, x), \quad (36)$$

giving the S-parameters $(S_{11,1}^{\text{meas}}, S_{21,1}^{\text{meas}})$ and $(S_{11,2}^{\text{meas}}, S_{21,2}^{\text{meas}})$, respectively. The first of these orientations is labeled 1 in Fig. 4. The second orientation corresponds to a rotation of the cube by 90° and is labeled 2 in Fig. 4. The measured S-parameters only implicate ε_B , μ_A , and μ_C , which can be found by solving the set of simultaneous equations,

$$S_{11,n}^{\text{thy}}(\varepsilon_B, \mu_A, \mu_C) - S_{11,n}^{\text{meas}} = 0, n = 1 \quad (37)$$

$$S_{21,n}^{\text{thy}}(\varepsilon_B, \mu_A, \mu_C) - S_{21,n}^{\text{meas}} = 0, n = 1, 2, \quad (38)$$

using Newton's method. Next, a measurement is made using orientation 3 in Fig. 4,

$$(A, B, C) \rightarrow (y, -x, z) \quad (39)$$

giving $(S_{11,3}^{\text{meas}}, S_{21,3}^{\text{meas}})$. This measurement implicates ε_A , μ_B , and μ_C . However, μ_C is now known, so ε_A and μ_B may be found by solving,

$$S_{11,3}^{\text{thy}}(\varepsilon_A, \mu_B) - S_{11,3}^{\text{meas}} = 0 \quad (40)$$

$$S_{21,3}^{\text{thy}}(\varepsilon_A, \mu_B) - S_{21,3}^{\text{meas}} = 0, \quad (41)$$

using Newton's method. Finally, a measurement is made under orientation 4 of Fig. 4,

$$(A, B, C) \rightarrow (z, x, y) \quad (42)$$

implicating ε_C , μ_A , and μ_B . Since both μ_A , and μ_B are now known, ε_C can be found by solving,

$$S_{21,4}^{\text{thy}}(\varepsilon_C) - S_{21,4}^{\text{meas}} = 0 \quad (43)$$

using Newton's method. Note that when both reflection and transmission data is available, but only one S-parameter is required, a choice is made to use transmission data since experience shows that it is more robust.

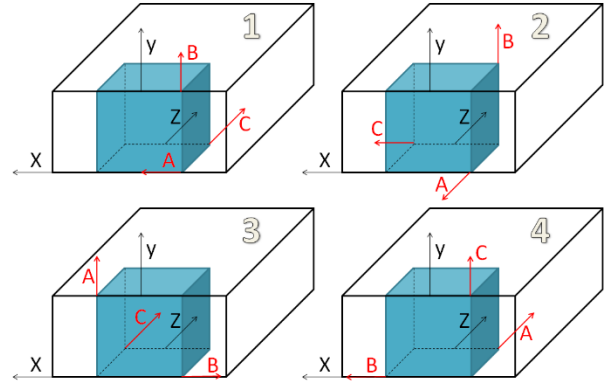


Fig. 4. Four cube orientations used in the three-step process.

IV. MEASURED RESULTS

A. Experimental setup

Demonstration of the partially-filled waveguide technique is undertaken by performing appropriate measurements at S-band and employing the extraction algorithm developed in the previous section. The waveguide system consists of two 5 inch (12.7 cm) long sections of WR-284 rectangular guide with coaxial transitions connected at the ends. These are attached through test port cables to an Agilent E5071C vector network analyzer (VNA); the assembled system is shown in Fig. 5. The VNA is calibrated at the open ends of the waveguide sections using a through-reflect-line (TRL) method. A cubical material sample is inserted in the end of one of the

waveguide sections so that its surface is flush to the open-ended waveguide surface and centered between the walls, as shown in Fig. 6. The two sections of guide are then assembled and the reflection coefficient S_{11} , and transmission coefficient, S_{21} , are measured. Assembly is done using precision alignment pins to ensure high repeatability between measurements. The measurement process is repeated with the sample inserted into the appropriate orientations described in section III. Note that the S-parameters must be phase corrected to account for the fact that the rear surface of the cube is not located at the calibration plane. All measurements were made with a -5dBm source power, 64 averages, and a 70 kHz IF bandwidth.

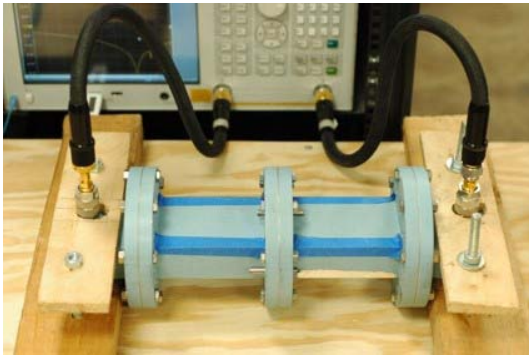


Fig. 5. Assembled S-band waveguide system.

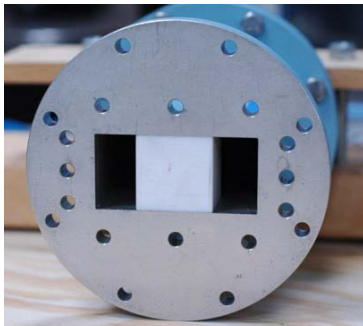


Fig. 6. Cubical sample inserted into waveguide section.

B. Experimental results

To test the characterization procedure using an anisotropic material, a cube was constructed by gluing together Rogers RO3010 circuit board substrate and Rogers RT/duroid 5870 substrate. The 3010 board has a thickness of $t_1 = 1.27$ mm, a dielectric constant of $\epsilon'_{r1} = 10.2$ and a loss

tangent of $\tan \delta_1 = 0.0022$. The 5870 board has a thickness of $t_2 = 3.4$ mm, a dielectric constant of $\epsilon'_{r2} = 2.33$, and a loss tangent of $\tan \delta_2 = 0.0012$. The resulting cube, shown in Fig. 7, has uniaxial dielectric properties and isotropic magnetic properties. If the B direction is chosen to be aligned perpendicular to the layer interfaces, then it is expected that ϵ_A and ϵ_C should be identical, but different from ϵ_B . The sample was constructed approximately 0.01 mm larger than the inner dimensions of the sample holder so that when inserted it would compress slightly and eliminate air gaps between the MUT and the sample holder walls.

The simple geometry of the uniaxial cube allows ϵ_A , ϵ_B , and ϵ_C to be estimated using closed-form expressions. At the highest frequency considered in the measurements, the free-space electrical length of the stack period is $k_0(t_1 + t_2) = 0.387$. Since $k_0\sqrt{\epsilon'_{r1}}(t_1 + t_2) \ll 2\pi$, the following approximate formulas may be used to determine the biaxial material constants [9],

$$\epsilon_B = \left[\frac{1}{\epsilon_{r2}} - \frac{\epsilon_{r1} - \epsilon_{r2}}{\epsilon_{r1}\epsilon_{r2}} \frac{t_1}{t_1 + t_2} \right]^{-1} \quad (44)$$

$$\epsilon_A = \epsilon_C = \epsilon_{r2} + (\epsilon_{r1} - \epsilon_{r2}) \frac{t_1}{t_1 + t_2} \quad (45)$$

where $\epsilon_{r1} = \epsilon'_{r1}(1 - j \tan \delta_1)$ and $\epsilon_{r2} = \epsilon'_{r2}(1 - j \tan \delta_2)$. Using the board parameters gives $\epsilon_B = 2.95 - j0.0038$ and $\epsilon_A = \epsilon_C = 4.47 - j0.0081$. Because of internal reflections, the results of [10] suggest deviations of up to 10% between these approximations and the values measured using the partially-filled waveguide. Also, the slight anisotropy of the boards themselves suggests that ϵ_A should differ slightly from ϵ_C [11].

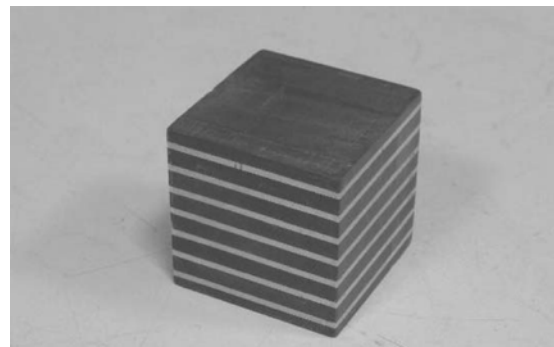


Fig. 7. Layered cube constructed from alternating layers of Rogers substrates.

The S-parameters of the uniaxial cube were measured 10 separate times, recalibrating between the measurements, and the material parameters were extracted using the 3-step procedure outlined in section III. The average values are shown in Figs. 8 and 9.

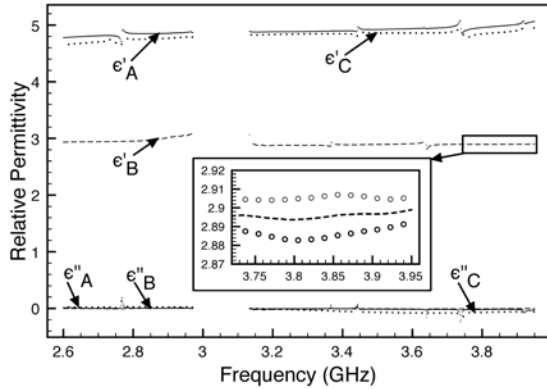


Fig. 8. Relative permittivities (mean values) of the uniaxial cube extracted using 10 measurement sets. Inset shows $2\text{-}\sigma$ confidence interval.

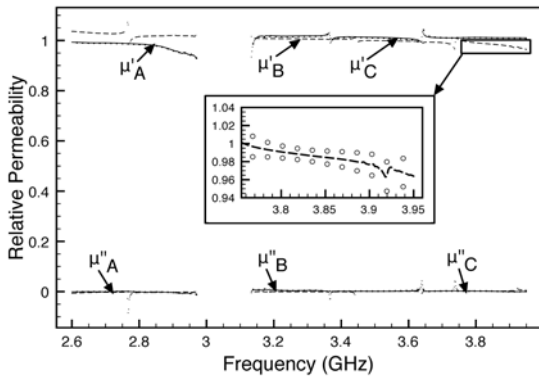


Fig. 9. Relative permeabilities (mean values) of the uniaxial cube extracted using 10 measurement sets. Inset shows $2\text{-}\sigma$ confidence interval.

The results for ϵ_A and ϵ_C are slightly higher than predicted by the closed-form expression (36), while ϵ_B is very close to the predicted value. The extracted values of μ_r are all close to unity, as expected, since the cube is non-magnetic. Note that the variance between measurement sets is quite small, such that showing the error bars in the figures would be distracting. Instead, the smaller insets in the figures show 95% ($2\text{-}\sigma$) confidence intervals for portions of the data sets; these intervals are typical across the entire frequency range.

The narrow confidence intervals suggest that noticeable variations in the extracted parameters are due to systematic errors, such as imperfect machining and alignment of the sample layers, or the presence of glue between sample layers, or air gaps between the sample and the waveguide walls, accentuated in certain frequency ranges by an ill-conditioning of the extraction process. This can be observed as gaps in the data in the frequency range 3 GHz - 3.15 GHz. There is amplified propagation of experimental uncertainties near frequencies where the sample is a half-wavelength long, a problem inherent to all guided-wave techniques in which both permittivity and permeability are determined (including the Nicolson-Ross-Wier closed-form method for isotropic materials [12-13]). Typically, the propagated error becomes so large that extraction is completely unreliable. This is a drawback of using a cubical sample holder, since the thickness of the material cannot be reduced below a half-wavelength. Experience has shown that a frequency range within approximately $\pm 5\%$ of the half-wavelength frequency should be avoided, and data within that range is not displayed in the figures, producing the observed gaps. It is possible, however, to interpolate the values of the parameters in the gaps. Figures 10 and 11 show the extracted parameters obtained by fitting a fifth-order polynomial to the data.

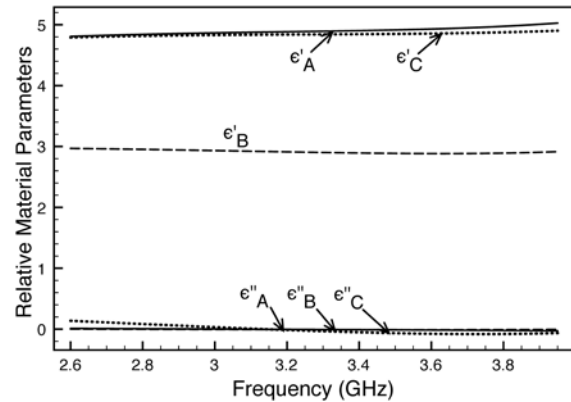


Fig. 10. Extracted relative permittivities of the uniaxial cube fitted to a fifth-order polynomial.

The extracted values of permittivity and permeability are quite similar to those obtained using the reduced-aperture waveguide described in [4]. To provide a direct comparison, the material

parameters ϵ_A and ϵ_B extracted using both methods are directly compared in Figs. 12 and 13, while a comparison for the parameter μ_A is shown in Fig. 14. Results for the parameters ϵ_C , μ_B , and μ_C are quite similar. Note that the reduced-aperture waveguide technique also has difficulties near half wavelength frequencies, but because the propagation constants of the modes are different than those for the partially-filled guide, the gaps appear in the range 3.55 GHz - 3.75 GHz, and do not coincide with those of Figs. 8 and 9. This suggests that combining data from both techniques may ameliorate the half-wavelength issue.

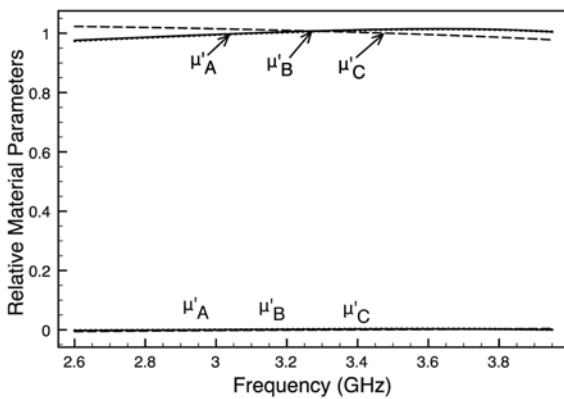


Fig. 11. Extracted relative permeabilities of the uniaxial cube fitted to a fifth-order polynomial.

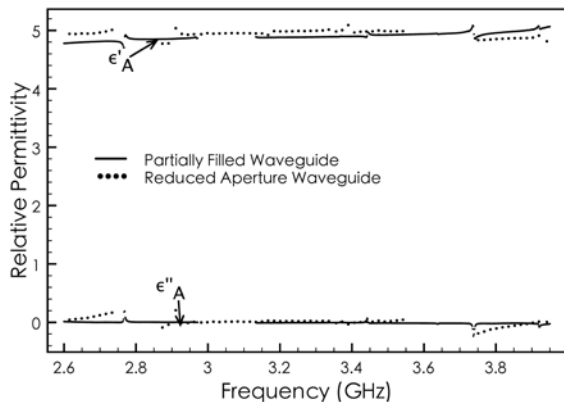


Fig. 12. Comparison of ϵ_A for the uniaxial cube extracted using the partially-filled waveguide technique and the reduced-aperture waveguide technique [4].

V. CONCLUSION

This paper introduces a method for measuring the electromagnetic properties of a biaxial material

using a partially-filled rectangular waveguide. The proposed technique is validated using experimental data, and its accuracy is found to be commensurate with that of the reduced-aperture waveguide technique, without the need for a special sample holder, and with less worry about air gaps between the sample and the waveguide walls. The drawback to the method is the need for a more complicated theoretical analysis. A combination of both techniques may provide a means for overcoming the difficulties with accurately extracting the parameters near frequencies where the sample is a half wavelength in thickness.

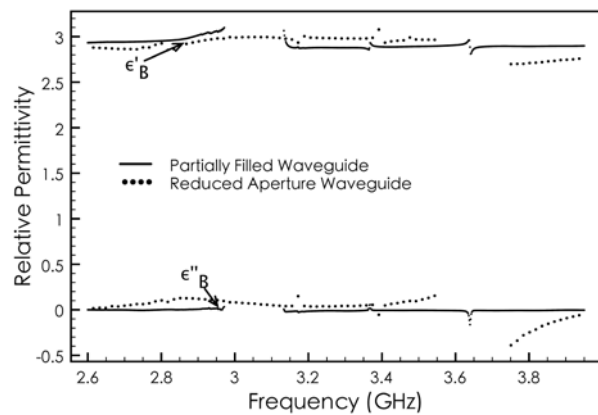


Fig. 13. Comparison of ϵ_B for the uniaxial cube extracted using the partially-filled waveguide technique and the reduced-aperture waveguide technique [4].

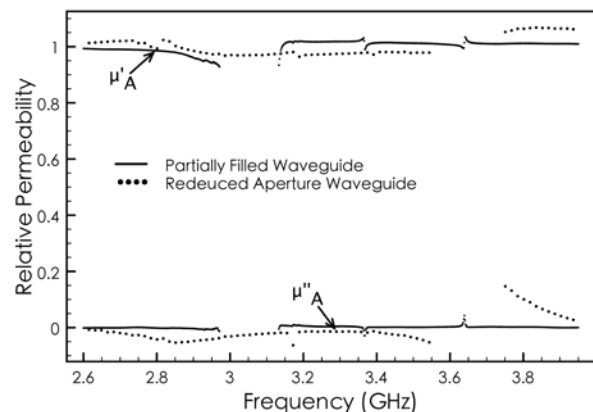


Fig. 14. Comparison of μ_A for the uniaxial cube extracted using the partially-filled waveguide technique and the reduced-aperture waveguide technique [4].

ACKNOWLEDGMENT

The research reported in this paper was supported by the US Air Force Office of Scientific Research under grant FA9550-09-1-0182.

REFERENCES

- [1] Y. Ma, P. Wang, X. Chen, and K. Ong, "Near-field plane-wave-like beam emitting antenna fabricated by anisotropic metamaterial," *Applied Physics Letters*, vol. 94, no. 4, pp. 044107, 2009.
- [2] G. Mumcu, K. Sertel, and J. Volakis, "Miniature antennas and arrays embedded within magnetic photonic crystals," *IEEE Antennas and Wireless Propagation Letters*, vol. 5, no. 1, pp. 168-171, Dec. 2006.
- [3] B. Crowgey, O. Tuncer, E. Rothwell, B. Shanker, and L. Kempel, "Development of numerical techniques for simulated characterization of anisotropic materials," *28th Annual Review of Progress in Applied Computational Electromagnetics (ACES)*, pp. 553-557, Columbus, Ohio, April 2012.
- [4] B. Crowgey, E. Rothwell, S. Balasubramaniam, L. C. Kempel, O. Tuncer, and M. Havrilla, "Characterization of biaxial anisotropic material using a reduced aperture waveguide," *IEEE AP-S International Symposium and URSI Radio Science Meeting*, Spokane, WA, July 3-8, 2011.
- [5] Á. Gómez, I. Barba, A. Cabeceira, J. Represa, G. Molina-Cuberos, M. Núñez, J. Margineda, Á. Vegas, and M. Solano, "Theoretical and experimental analysis of rectangular waveguides with isotropic chiral media," *23rd Annual Review of Progress in Applied Computational Electromagnetics (ACES)*, pp. 1140-1144, Verona, Italy, March 2007.
- [6] S. Ramo, J. Whinnery, and T. Duzer, *Fields and Waves in Communications Electronics*, 3rd ed., John Wiley & Sons, New York, 1994.
- [7] B. Crowgey, R. Ouedraogo, E. Rothwell, L. Kempel, and S. Balasubramaniam, "Measurement of the electromagnetic properties of biaxial anisotropic materials using a waveguide technique," *Inverse Problems Symposium (IPS)*, East Lansing, MI, June 2010.
- [8] A. Bogle, M. Havrilla, D. Nyquist, L. Kempel, and E. Rothwell, "Electromagnetic material characterization using a partially-filled rectangular waveguide," *J. Electromagnetic Waves Applications*, vol. 19, no. 10, pp. 1291-1306, 2005.
- [9] R. Collin, "A simple artificial anisotropic dielectric medium," *IRE Transaction on Microwave Theory and Techniques*, pp. 206 - 209, April 1958.
- [10] D. Killips, L. Kempel, D. Nyquist, and E. Rothwell, "Analysis of layering dielectrics on

effective permittivity using wave matrices," *IEEE Antennas and Propagation Society International Symposium*, Washington, D.C., vol. 3A, pp. 212-215, July 3-8, 2005.

- [11] J. Rautio, "Measurement of uniaxial anisotropy in Roger RO3010 substrate material," *COMCAS*, 2009.
- [12] A. Nicolson and G. Ross, "Measurement of the intrinsic properties of materials by time-domain techniques," *IEEE Trans. Instrum. Meas.*, vol. 19, no. 4, pp. 377-382, Nov. 1970.
- [13] W. Weir, "Automatic measurement of complex dielectric constant and permeability at microwave frequencies," *Proc. IEEE*, vol. 62, no. 1, pp. 33-36, Jan. 1974.



Junyan Tang was born in Hangzhou, China in 1986. He received the B.S. degree from Zhejiang University, Hangzhou, China, and the M.S. degree in electrical engineering from Michigan State University, East Lansing, MI. He is currently working toward the Ph.D. degree at Michigan State. His research interests include metamaterials, antennas and material characterization.



Benjamin R. Crowgey was born in Iron River, MI, on July 17, 1985. He received the B.S. degree and M.S. degree in electrical engineering from Michigan State University, East Lansing, in 2007 and 2009, respectively. He is currently working on his Ph.D. at Michigan State University with a current expected date of graduation during summer of 2013.

His current research interests include anisotropic material characterization, self-structuring antennas, traveling wave antennas, electromagnetic radiation, and scattering.



Ozgur Tuncer received the B.Sc. degree in electrical and electronics engineering from the Middle East Technical University, Ankara, Turkey, in 2003, the M.Sc. degree in electrical engineering and information technology from the Technische Universität München

Munich, in 2005, and the Ph.D. degree in electrical engineering from Michigan State University, East Lansing, in 2012.

In 2006, he worked as a system engineer at Infineon Technologies, Munich, on the modelling of 3G mobile communication products for HSDPA/HSUPA. From 2007 to 2012, he was a research assistant at Michigan State, where he worked on the development of the generalized finite element methods. He is currently working at ANSYS as a research and development engineer. His research interests include all aspects of theoretical and computational electromagnetics, particularly the finite element methods.



Edward J. Rothwell was born in Grand Rapids, MI, on September 8, 1957. He received the B.S. degree in electrical engineering from Michigan Technological University, Houghton, in 1979, the M.S. degree in electrical engineering and the degree of electrical engineer from Stanford University, Stanford, CA, in 1980 and 1982, and the Ph.D. degree in electrical engineering from Michigan State University, East Lansing, MI, in 1985, where he held the Dean's Distinguished Fellowship.

He worked for Raytheon Co., Microwave and Power Tube Division, Waltham, MA, from 1979-1982 on low power traveling wave tubes, and for MIT Lincoln Laboratory, Lexington, MA, in 1985. He has been at Michigan State University from 1985-1990 as an assistant professor of electrical engineering, from 1990-1998 as an associate professor, and from 1998 as professor. He is co-author of the book *Electromagnetics* (Boca Raton, FL: CRC Press, 2001; 2nd edition 2008). His current interests include electromagnetic theory, antennas, and material characterization.

Dr. Rothwell received the John D. Withrow award for teaching excellence from the College of Engineering at Michigan State University in 1991, 1996, 2006, and 2012, the Withrow Distinguished Scholar Award in 2007, the MSU Alumni Club of Mid Michigan Quality in Undergraduate Teaching Award in 2003, and the MSU Distinguished Faculty Award in 2013. He was a joint recipient of the Best Technical Paper Award at the 2003 Antenna Measurement Techniques Association Symposium, and in 2005 he received the Southeast Michigan IEEE Section Award for Most Outstanding Professional. He is a member of Phi Kappa Phi, Sigma Xi, ACES, and Commission B of URSI, and is a Fellow of the IEEE.



B. Shanker received his B'Tech degree from the Indian Institute of Technology, Madras, India in 1989, and the M.S. and Ph.D degrees in 1992 and 1993, respectively, from the Pennsylvania State University. From 1993 to 1996 he was a research associate in the Department of Biochemistry and Biophysics at Iowa State University where he worked on the Molecular Theory of Optical Activity. From 1996 to 1999 he was with the Center for Computational Electromagnetics at the University of Illinois at Urbana-Champaign as a Visiting Assistant Professor, and from 1999-2002 with the Department of Electrical and Computer Engineering at Iowa State University as an Assistant Professor. Currently, he is a Professor in the Department of Electrical and Computer Engineering at Michigan State University.

He has authored/co-authored over 300 journal and conferences papers and presented a number of invited talks. His research interest include all aspects of computational electromagnetics (frequency and time domain integral equation based methods, multi-scale fast multipole methods, fast transient methods, higher order finite element and integral equation methods), propagation in complex media, mesoscale electromagnetics, and particle and molecular dynamics as applied to multiphysics and multiscale problems.

Dr. Shanker was an Associate Editor for IEEE Antennas and Wireless Propagation Letters (AWPL), is an Associate Editor for IEEE Transactions on Antennas and Propagation, and is a full member of the USNC-URSI Commission B. He is Fellow of IEEE, elected for his contributions in computational electromagnetics. He has also been awarded the Withrow Distinguished Junior scholar (in 2003), Withrow Distinguished Senior scholar (in 2010) and the Withrow teaching award (in 2007).



Leo C. Kempel was born in Akron, OH, in October 1965. He earned his B.S.E.E. at the University of Cincinnati in 1989 as well as the M.S.E.E. and Ph.D. degrees at the University of Michigan in 1990 and 1994, respectively.

After a brief Post-Doctoral appointment at the University of Michigan, Dr. Kempel joined Mission Research Corporation in 1994 as a Senior Research Engineer. He led several projects involving the design of conformal antennas, computational electromagnetics, scattering analysis, and high power/ultrawideband microwaves. He joined Michigan State University in

1998. Prof. Kempel's current research interests include computational electromagnetics, conformal antennas, microwave/millimeter wave materials, mixed-signal electromagnetic interference techniques, and measurement techniques. Prof. Kempel has been awarded a CAREER award by the National Science Foundation and the Teacher-Scholar award by Michigan State University in 2002. He also received the MSU College of Engineering's Withrow Distinguished Scholar (Junior Faculty) Award in 2001. He served as an IPA with the Air Force Research Laboratory's Sensors Directorate from 2004-2005 and 2006-2008. He was the inaugural director of the Michigan State University High Performance Computing Center. He was the first Associate Dean for Special Initiatives in the College of Engineering at Michigan State University for 2006-2008 and is now serving as the Associate Dean for Research, also in the College of Engineering at Michigan State University. He was appointed to the US Air Force Scientific Advisory Board in October 2011.

Dr. Kempel served as the technical chairperson for the 2001 Applied Computational Electromagnetics Society (ACES) Conference and technical co-chair for the Finite Element Workshop held in Chios, GREECE in 2002. He was a member of the Antennas and Propagation Society's Administrative Committee and was a member of the ACES Board of Directors. He served as an Associate Editor for the *IEEE Transactions on Antennas and Propagation*. He is currently the Fellow Evaluation Committee Chairperson for the IEEE Antennas and Propagation Society. He is an active reviewer for several IEEE publications as well as JEW and Radio Science. He co-authored *The Finite Element Method for Electromagnetics* published by IEEE Press. Dr. Kempel is a member of Tau Beta Pi, Eta Kappa Nu, and Commission B of URSI, and is a Fellow of the IEEE.



Michael J. Havrilla received B.S. degrees in Physics and Mathematics in 1987, the M.S.E.E degree in 1989 and the Ph.D. degree in electrical engineering in 2001 from Michigan State University, East Lansing, MI. From 1990-1995, he was with

General Electric Aircraft Engines, Evendale, OH and Lockheed Skunk Works, Palmdale, CA, where he worked as an electrical engineer. He is currently a Professor in the Department of Electrical and Computer Engineering at the Air Force Institute of Technology, Wright-Patterson AFB, OH.

He is a member of URSI Commission B, a senior member of the IEEE, and a member of the Eta Kappa Nu and Sigma Xi honor societies. His current research interests include electromagnetic and guided-wave theory, electromagnetic propagation and radiation in complex media and structures and electromagnetic materials characterization.